VIRTUAL PHOTON MEASUREMENTS WITH HADES AT GSI*

Jan-Hendrik Otto

for the HADES Collaboration

II. Physikalisches Institut, Justus-Liebig Universität Gießen, Germany

Received 29 July 2022, accepted 12 September 2022, published online 14 December 2022

In this work, we present preliminary results of HADES on the dielectron analysis of 4.5 billion Ag+Ag collisions ((0–40)% centrality) at a centre-of-mass energy of $\sqrt{s_{NN}} = 2.55$ GeV. The obtained dielectron signal spectrum is compared to a simulated hadronic cocktail and nucleon–nucleon reference spectra revealing a strong in-medium contribution quantified by the dielectron excess ratio R_{AA}. The average temperature of the collision system can be extracted from the slope of the in-medium contribution. In a momentum differential analysis, we observe modifications of the dielectron signal shape in the ω–ρ invariant mass region.

DOI:10.5506/APhysPolBSupp.16.1-A131

1. Introduction

The **H**igh **A**cceptance **D**i**E**lectron **S**pectrometer (HADES) [1] is dedicated to the measurement of electromagnetic and rare hadronic [2] probes from elementary to heavy-ion collisions and to study the in-medium behaviour of dileptons, as their spectral distributions reveal the thermal properties of the medium. In heavy-ion collisions at $\sqrt{s_{NN}} = 2$–3 GeV as measured with HADES, matter is compressed to 2-3 times the groundstate density and heated up to temperatures of about $T = 70$ MeV [3], thus HADES is investigating the moderate temperature and high-density region of the QCD phase diagram. Intriguingly, in neutron star mergers, the conditions are believed to be very similar [4].

2. The HADES experiment

HADES is a fixed target experiment located at the SIS 18 accelerator at GSI, Germany. HADES is built as a magnet spectrometer covering nearly the full forward hemisphere apart from small polar angles. Four layers of low

* Presented at the 29$^{\text{th}}$ International Conference on Ultrarelativistic Nucleus–Nucleus Collisions: Quark Matter 2022, Kraków, Poland, 4–10 April, 2022.

mass **M**ini-**D**rift-**C**hambers (MDCs) located in front (2) and two behind (2) the magnetic field region provide tracking information. The time-of-flight measurement is performed by **R**esistive **P**late **C**hambers (RPCs) and a ToF wall at polar angles of 18°–44° and 44°–88°, respectively. A hadron blind **R**ing **I**maging **CH**erenkov detector (RICH) considerably enhances electron identification. Recently, the RICH detector has been upgraded with a new photon detector consisting of 428 64-channel H12700 **M**ulti-**A**node PMTs (MAPMTs) with FPGA-based readout [5]. Furthermore, an electromagnetic calorimeter has been added covering only a fraction of the total HADES acceptance yet.

3. Electron identification and pair invariant mass spectrum

In this report, 4.5 billion Ag+Ag collisions at 1.58 A GeV beam energy and ((0–40)%) centrality selection are analyzed. In HADES, electrons are identified with high efficiency and purity. Possible pion contamination arises from randomly matched pion tracks with RICH rings. The pion suppression factor determined in simulation is of the order of 10^5 and even higher for $p < 400$ MeV/c. The electron purity is estimated using UrQMD [6] and an experimental RICH-rotation technique to be above 99%. In the future, this will be further improved with a fully equipped electromagnetic calorimeter. Electrons produced in photon conversion processes are efficiently detected and removed from the sample using the RICH by either the detection of double rings or the amount of measured Cherenkov photons if the rings fully overlap, see also [7] for a more detailed insight.

The combinatorial background arising in the pairing of electrons and positrons can be described by the geometrical mean of the same-event e^+e^+ and e^-e^- pairs ($\langle FG_{++}\rangle, \langle FG_{--}\rangle$) weighted with the so-called *k-factor*. This accounts for acceptance and reconstruction differences in the pairings and is derived using the event-mixing technique, see formula (1) [8]. Within the event mixing, electrons and positrons reconstructed in different events are paired ($\langle fg_{+-}\rangle$, $\langle fg_{++}\rangle, \langle fg_{--}\rangle$), which allows for almost unlimited statistics

$$\langle BG_{+-}\rangle = k \times 2\sqrt{\langle FG_{++}\rangle\langle FG_{--}\rangle} \quad \text{with} \quad k = \frac{\langle fg_{+-}\rangle}{2\sqrt{\langle fg_{++}\rangle\langle fg_{--}\rangle}}\,. \tag{1}$$

This same-event like-sign combinatorial background evaluation is used for low invariant masses $M_{ee} < 300$ MeV/c^2. For larger masses, the background is obtained from mixed events only in order to reduce statistical errors. Normalization to the same-event background is obtained in the region 300 MeV/$c^2 < M_{ee} \leq 700$ MeV/c^2. The resulting invariant mass distribution in the HADES acceptance is shown in Fig. 1. An efficiency correction is applied based on single leptons and is derived by embedding simulated electrons with momenta up to $p_e = 1.5$ GeV$/c$ into real data.

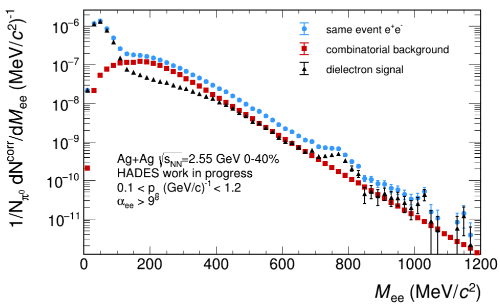

Fig. 1. Efficiency corrected invariant mass spectrum.

The corresponding single lepton efficiency exceeds $\epsilon = 50\%$ over the whole momentum range and reaches up to $\epsilon \sim 80\%$ at small momenta. The invariant mass spectrum is restricted to single lepton momenta of 100 MeV$/c <$ $p_e <$ 1200 MeV$/c$ and pair opening angles $\alpha > 9°$. In the ρ–ω mass region a clear enhancement above the exponential slope is visible and pairs up to the ϕ-meson pole mass are reconstructed. The signal-to-background ratio surpasses 1 for $M_{ee} > 500$ MeV$/c^2$ and reaches up to 3 at around the ω-meson pole mass.

4. Decomposition of the dielectron signal

The obtained dielectron signal is composed of contributions from all stages of the evolution of the collision system, namely the initial NN collisions, the hot and dense phases of the fireball and, finally, the decay of hadrons at freeze-out. In order to describe the latter, simulations of the relevant hadronic sources are performed utilizing the software package Pluto [9]. The π^0 and η multiplicities are extracted from an analysis of the $\pi^0/\eta \to \gamma\gamma^{(\star)} \to 4e$ decay pattern, while the ω and ϕ mesons are studied in their e^+e^- and K^+K^- decay channel, respectively. These contributions are shown together with the dielectron signal spectrum in Fig. 2, where the current systematic error in the η multiplicity of 30% is indicated by the broad band. The initial NN contribution can either be measured with $p{+}p$ and $p{+}n$ collisions, however, recently taken HADES data (Febuary–March 2022) are currently analyzed. Or the contribution is estimated from models, here GiBUU [10] is used (release 2021), modeling the NN reference as $NN = 0.54\,pp + 0.46\,pn$ [3]. Bremsstrahlung and the $\Delta \to Ne^+e^-$ channel are included in Fig. 2 from simulation as in [11].

The dielectron spectrum shows a strong excess over the whole invariant mass region to the simulated sources. This excess is identified as the in-medium radiation emitted from the hot and dense phases of the collision.

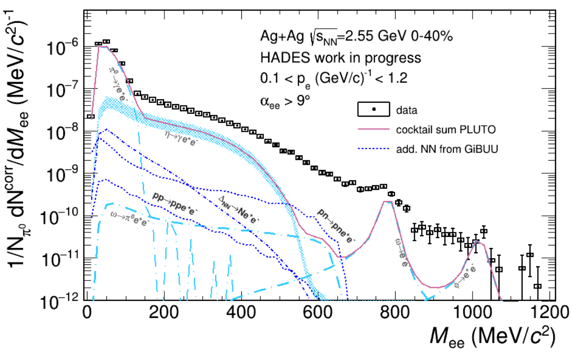

Fig. 2. Dielectron signal together with the hadronic feeze-out cocktail obtained from Pluto [9] simulation and the initial NN contributions from the GiBUU model [10].

5. The dielectron excess ratio R_{AA}.

The excess in the dielectron yield can be quantified by the dielectron excess ratio R_{AA}, normalizing the obtained dielectron spectrum to the one from elementary reactions, where no in-medium contribution is present. Due to the lack of an NN reference at the same energy, a measurement at $\sqrt{s_{NN}} = 2.42$ GeV [3] is used with the $\eta \to e^+e^-\gamma$ contribution being subtracted in both data sets to account for the different energy. The resulting R_{AA} is shown in Fig. 3 together with data obtained in Au+Au [3] and Ar+KCl [12] collisions. The uncertainty in the η multiplicity is indicated by the yellow/grey band. While a slight excess above unity is observed at small invariant masses, the R_{AA} strongly rises beyond the π^0-Dalitz region to a mean value of $R_{AA} \approx 3$. According to the system size, the Ag+Ag data aligns in between the Au+Au and Ar+KCl measurements.

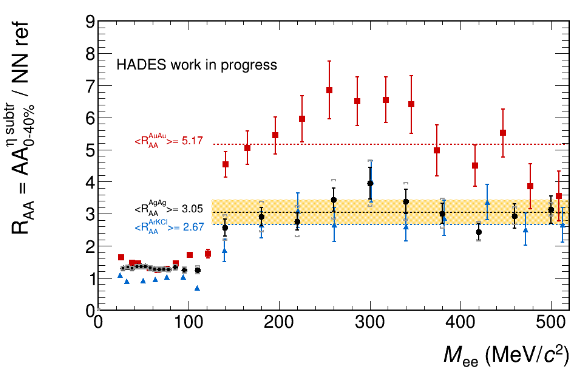

Fig. 3. (Color online) The dielectron excess ratio R_{AA} in Ag+Ag collisions at $\sqrt{s_{NN}} = 2.55$ GeV in comparison to Au+Au at $\sqrt{s_{NN}} = 2.55$ GeV [3] and Ar+KCl data at $\sqrt{s_{NN}} = 3.18$ GeV [12] measured by HADES.

6. Temperature estimation of the fireball

The in-medium contribution to the obtained dielectron signal spectrum is isolated subtracting the initial NN simulated by GiBUU and the hadronic freeze-out contributions (Fig. 2) from the full spectrum (Fig. 1). Figure 4 shows the remaining in-medium contribution — the temperature is extracted from the inverse slope. It is estimated to $kT = 77.9^{+3.7}_{-3.0}$ MeV with the combined error dominated by the uncertainty in the η multiplicity. The value is as expected slightly higher wrt the temperature measured in Au+Au by HADES at $\sqrt{s_{NN}} = 2.42$ GeV [3].

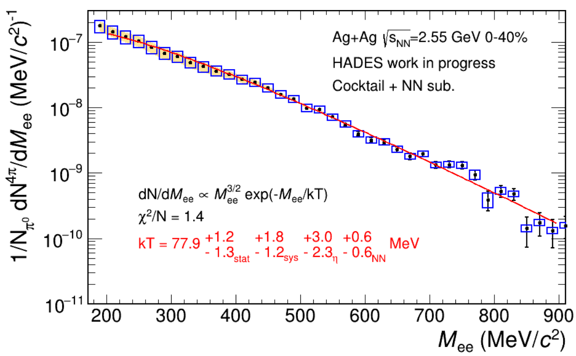

Fig. 4. Extraction of the mean in-medium temperature applying a thermal fit to the in-medium dielectron signal.

7. Momentum differential analysis

A momentum differential analysis of the dielectron production is shown in Fig. 5 in three bins of pair momentum. In the small ($0 < p_{ee}$ (GeV$/c)^{-1} \leq 0.6$) and medium ($0.6 < p_{ee}$ (GeV$/c)^{-1} \leq 1.2$) momentum bin, a broad excess above a thermal continuum fit in the ρ–ω mass region is seen, which turns into a clear peak structure in the high momentum bin. Two scenarios are conceivable: First, in the low momentum data, the peak structure from the $\omega \to e^+e^-$ decay may be hidden under a broad excess linked to the $\rho \to e^+e^-$ channel in the low momentum data. Comparing to Pluto simulation, this interpretation would require ω-melting for low momenta compared to thermal production scenarios. Second, the $\omega \to e^+e^-$ signal itself might be broadened in the low momentum data. To conclude and validate one of these interpretations in future, a precise knowledge of the $\rho \to e^+e^-$ line shape is required from simulation.

8. Summary

New dielectron spectra of the HADES Collaboration for Ag+Ag collisions at $\sqrt{s_{NN}} = 2.55$ GeV show an unprecedented quality in terms of

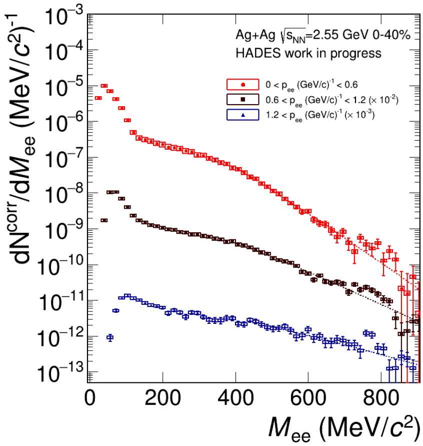

Fig. 5. Dielectron spectra in three bins of pair momentum.

statistics and S/B ratio. Excess radiation beyond the NN reference has been measured to $R_{AA} \approx 3$ for $M_{ee} > M_{\pi^0}$ and the mean medium temperature is estimated to $kT = 77.9^{+3.7}_{-3.0}$ MeV. A pair momentum differential analysis shows a modification of the dielectron signal in the ρ–ω-invariant mass region.

This work was supported by HGS HiRE, GSI and the BMBF, grant No. 05P21RGFC1, 05P19RGFCA.

REFERENCES

[1] HADES Collaboration (G. Agakishiev *et al.*), *Eur. Phys. J. A* **41**, 243 (2009).

[2] HADES Collaboration (J. Adamczewski-Musch *et al.*), *Phys. Lett. B* **778**, 403 (2018).

[3] HADES Collaboration, *Nat. Phys.* **15**, 1040 (2019).

[4] M. Hanauske *et al.*, *J. Phys.: Conf. Ser.* **878**, 012031 (2017).

[5] C. Pauly *et al.*, The 9th International Workshop on Ring Imaging Cherenkov Detectors (RICH2016), Lake Bled, Slovenia, 5–9 September, 2016.

[6] S.A. Bass *et al.*, *Prog. Part. Nucl. Phys.* **41**, 255 (1998).

[7] HADES Collaboration (J.-H. Otto *et al.*), *PoS* **PANIC2021**, 235 (2022).

[8] PHENIX Collaboration (A. Adare *et al.*), *Phys. Rev. C* **81**, 034911 (2010).

[9] I. Fröhlich *et al.*, *PoS* **ACAT**, 076 (2007).

[10] O. Buss *et al.*, *Phys. Rep.* **512**, 1 (2012).

[11] A.B. Larionov, U. Mosel, L. von Smekal, *Phys. Rev. C* **102**, 064913 (2020).

[12] HADES Collaboration (G. Agakishiev *et al.*), *Phys. Rev. C* **84**, 014902 (2011).